Performance Limits of Low Bandgap Thermophotovoltaic Antimonide-Based Cells for Low Temperature Radiators

J.M. Borrego [1,2], C.A.Wang[3], P.S. Dutta [1,2], G.Rajagopalan[1], R.J. Gutmann [1,2], I.B. Bhat [1,2], H. Ehsani [4], J.F.Beausang[4], G. Nichols [4], and P.F. Baldasaro [4]

[1] *Center for Integrated Electronics and Electronics Manufacturing*
[2] *Department of Electrical, Computer and Systems Engineering*
Rensselaer Polytechnic Institute, Troy, NY – 12180
[3] *Lincoln Laboratory, Massachusetts Institute of Technology, Lexington, MA -02420*
[4] *Lockheed Martin Inc., Schenectady, NY – 12301*

Abstract. This paper assesses the performance of antimonide-based thermophotovoltaic cells fabricated by different technologies. In particular, the paper compares the performance of lattice matched quaternary (GaInAsSb) cells epitaxially grown on GaSb substrates to the performance of ternary (GaInSb) and binary (GaSb) cells fabricated by Zn diffusion on bulk substrates. The focus of the paper is to delineate the key performance advantages of the highest performance-to-date of the quaternary cells to the performance of the alternative ternary and binary antimonide-based diffusion technology. The performance characteristics of the cells considered are obtained from PC-1D simulations using appropriate material parameters.

INTRODUCTION

In order for Thermophotovoltaic (TPV) cells to be commercially viable it is necessary that they can be fabricated by processes that give cells with relatively good performance and with reproducible characteristics in semiconductor materials with energy band gaps in the range between 0.7 eV and 0.5 eV. At the present time the following fabrication process are being used when the material used is Sb based: molecular beam epitaxy (MBE), organometallic vapor phase epitaxy OMVPE and bulk diffusion. Recent work in our laboratory has shown that it is possible to fabricate GaSb and ternary GaInSb TPV cells in which the material has been grown by a Bridgman type technique and then the cell emitter is obtained by low temperature Zn diffusion. This fabrication process is inexpensive and has shown to produce cells with very reproducible characteristics. MBE and OMVPE are complex fabrication processes that have the advantage of giving cells

CP653, *Thermophotovoltaic Generation of Electricity: 5th Conference*
edited by T. J. Coutts, G. Guazzoni, and J. Luther

in which the physical structure and the doping concentration of the material in several regions can be tailored to achieve high performance cells. It is the purpose of this paper to present the results of computer simulations using PC-1D of the performance of Zn bulk diffused GaSb and GaInSb TPV cells and compare them to the performance of quaternary OMVPE grown cells as function of radiator temperature.

MATERIAL PARAMETERS

Computer simulations using PC-1D require a large number of material parameters that can be grouped as energy band parameters, carrier mobility parameters, optical parameters and recombination parameters. The energy band parameters of the III-V compounds have been compiled by Madelung (1). The mobility dependence upon carrier concentration for III-V binaries GaAs, GaSb, InAs and InSb has been reported in several papers (2,3,4). Optical constants of all the binary III-V compounds have been recently compiled (5). Experimental values of similar material parameters for the ternaries GaInSb and quaternaries GaInAsSb have not been reported. They can be estimated with confidence, from the corresponding material parameters of the binaries GaAs, InAs, GaSb and InSb, using equations developed by Adachi (6) and we have used that procedure for estimating those parameters for GaInAs and GaInAsSb alloys with band gaps in the range of 0.60 eV to 0.50 eV.

Figure 1 shows the measured mobility of electrons and holes in OMVPE grown quaternary material GaInAsSb with a bandgap of 0.55 eV and compares it with the mobility calculated using Matthiessen rule starting from the experimental mobility of the binaries GaAs, InAs, GaSb and InSb.

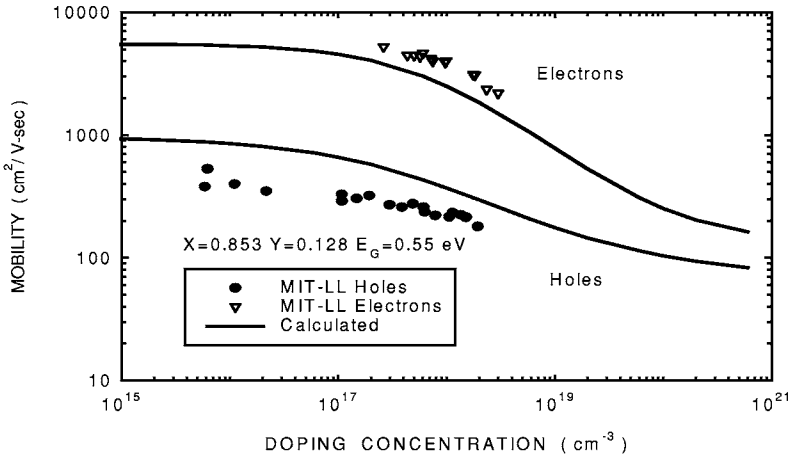

FIGURE 1. Electron and Hole Mobility of GaInAsSb Alloy.

The agreement between the experimental values and the calculated values is rather good considering the many assumptions used in obtaining the mobility of the alloy using Matthiessen rule. Similarly good agreement has been found between the measured optical absorption constant of the quaternary alloy GaInAsSb and the one calculated from the absorption constant of the binaries (7). Figure 2 shows a comparison between the calculated and the measured absorption constant for a GaInAsSb quaternary alloy of 0.53 eV bandgap (7).

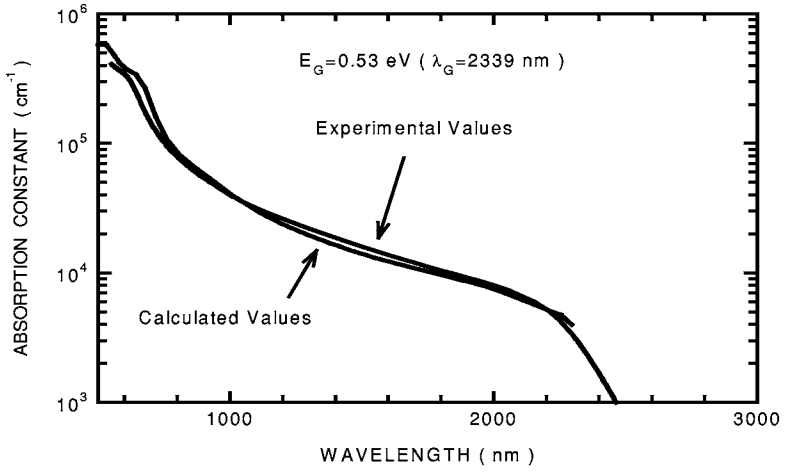

FIGURE 2. Optical Absorption Constant of GaInAsSb Alloy.

The recombination parameters are SRH, radiative or band-to-band and Auger recombination. Of these recombination processes, SRH cannot be estimated a priori since it is dependent upon the recombination centers introduced during the fabrication process. On the other hand, radiative and Auger recombination parameters can be calculated from the known band structure of the material. Recently Grein et al (8) have reported the use of accurate **K·p** band structures to obtain radiative, electron-electron, hole-hole and band-to-band Auger recombination rates in InAs/InGaSb long wavelength detectors. Using this paper as basis plus a recent compilation of Auger recombination coefficients for many semiconductors (9), we have estimated the recombination parameters for GaInSb and GaInAsSb alloys with band gaps of 0.50, 0.55 and 0.60 eV and the values of the radiative recombination coefficient B and of the Auger coefficients C_N and C_P are given below in Table 1.

TABLE 1. Radiative and Auger Recombination Coefficients

Bandgap (eV)	B (cm^3/sec)	C_N (cm^6/sec)	C_P (cm^6/sec)
0.60	8.2×10^{-11}	7.4×10^{-28}	7.5×10^{-28}
0.55	7.6×10^{-11}	1×10^{-27}	1.3×10^{-27}
0.50	6.9×10^{-11}	1.5×10^{-27}	2.6×10^{-27}

There is a question about the accuracy of these values as well as if they agree with measured values in these alloys, but at the present there are not reliable measurements and work is in progress to measure these coefficients. We believe the values of the Auger coefficients in Table 1 are accurate within a factor of 3 or 4 and have used them in simulations using PC-1D.

STRUCTURE OF SIMULATED Zn DIFFUSED CELLS

The physical structure of the simulated cells is very simple; it consists of a bulk wafer of binary GaSb or ternary GaInSb n-type material in which a p-type emitter has been formed by Zn diffusion at low temperature. A typical SIMS Zn diffusion profile in bulk GaInSb is shown in Fig. 3.

The profile shows that there is a high Zn concentration at the surface, around 10^{19} cm^{-3}, which is followed by a relatively slow exponential decay in the doping concentration with distance to $5x10^{18}$ cm^{-3} at 0.25 microns and then it decreases very sharply to a concentration to around 10^{16} cm^{-3} at 0.3 microns. Figure 3 shows that the doping concentration in the emitter is larger than 10^{18} cm^{-3} so the recombination in the emitter is dominated by Auger recombination and this cannot be changed as long as the emitter is formed by Zn diffusion.

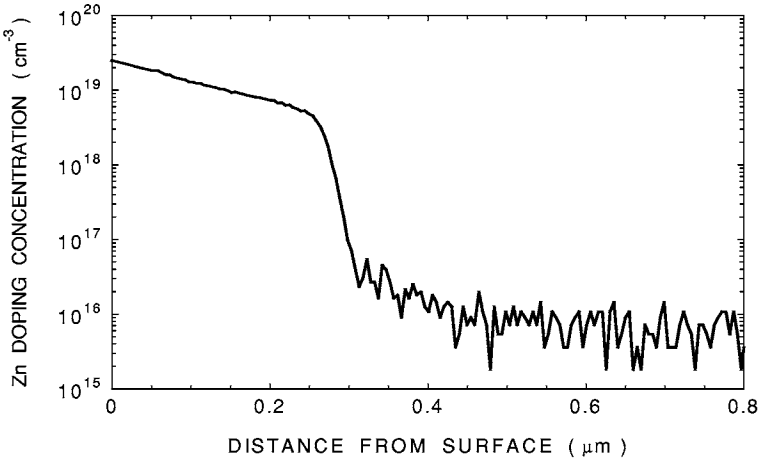

FIGURE 3. SIMS Emitter Doping Profile of Zn Bulk Diffused Cells

In order to achieve a high open circuit voltage, the doping concentration in the base should be chosen such that the recombination is mainly radiative. This implies low doping concentration but high enough so the PN junction has an adequate built-in voltage that allows carrier collection near open circuit conditions. This last condition can be achieved by doping the N-base at a concentration comparable to the conduction band density of states. In these low band gap materials the conduction band density of states is of the order of 10^{17}

cm^{-3} so the doping in the N-base should be within the range of 10^{16} cm^{-3} to 10^{17} cm^{-3}. As a starting design point we have chosen a doping concentration of $1x10^{17}$ cm^{-3} for the N-base of all the simulated cells since it is very difficult to obtain GaSb and GaInSb bulk material with lower doping concentration due to the native defects present.

For simulation purposes we have chosen the TPV cells to have a total area of 1 cm^2 and a thickness of 100 microns. The surface recombination in the front free surface is assumed to be 10^6 cm/sec. We have found that this value matches reasonably well the measured external quantum efficiency at short wavelengths. In the simulation we have assumed the metallic grid to form a perfect ohmic contact with the P-type emitter with a 10% obscuration ratio. Since the cell thickness is 100 microns and the diffusion length in the base is a few microns, the surface recombination velocity in the back surface is not relevant and for simulation purposes we have assumed to have a value of 10^7 cm/sec. Besides the above assumptions, the simulations do not include any effects due to photon recycling nor effects due to series resistance of the metallic grid in the TPV cell.

SIMULATION RESULTS FOR GaSb AND GaInSb TPV CELLS

Figure 4 shows the internal and external quantum efficiency, as well as the reflectance, of a GaInSb TPV cell with an energy bandgap of 0.55 eV using PC-1D to simulate the performance of the cell. The low internal QE at short wavelengths is caused by the high recombination in the heavily doped emitter . At longer wavelengths, the internal QE does not rise above 70% because of the long base and short diffusion length.

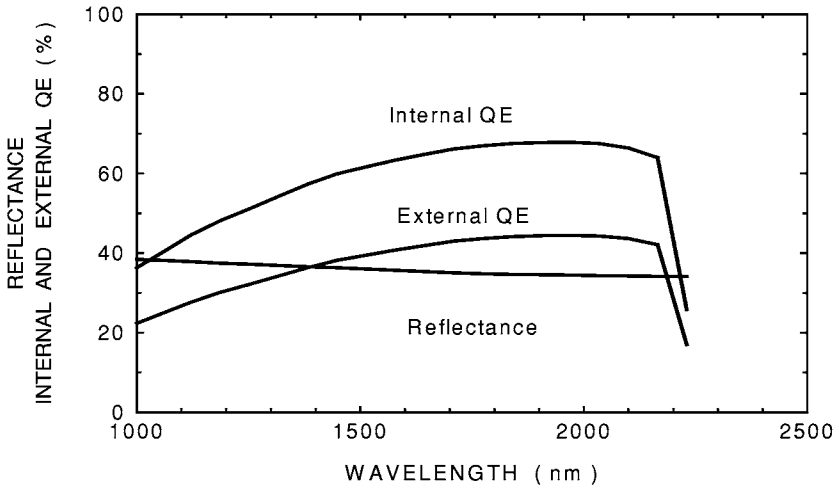

FIGURE 4. Simulation of Internal and External QE of GaInSb (0.55 eV) Cell.

Minority carrier's photogenerated in the base may diffuse toward the junction and collected or they diffuse away from the junction and are lost by bulk recombination that is predominantly Auger recombination. Besides the above simulations, we have determined the maximum power output performance of the Zn diffused cells as function of radiator temperature. The maximum power as function of Black Body radiator temperature for the several Zn diffused GaSb and GaInSb TPV cells is shown in Fig.5.

Figure 5 shows that in spite of the low radiator temperatures, the GaSb TPV cell always produces the largest output power. The reason for this surprising result is that the Auger recombination coefficients increase exponentially as the band gap decreases which causes an exponential increase in the dark current and a large decrease in the open circuit voltage. The increase in short circuit current with decreasing band gap does not compensate for the large decrease in open circuit voltage. In order to increase the performance of the low band gap GaInSb TPV cells it is necessary to lower the doping concentration in the N-base to a value in the range between 10^{16} cm^{-3} to 10^{17} cm^{-3} which may or may not be possible. This makes the recombination process in the base to be mainly radiative and also increases the value of the lifetime and diffusion length in the base bringing an increase in the QE and also lowering the cell dark current.

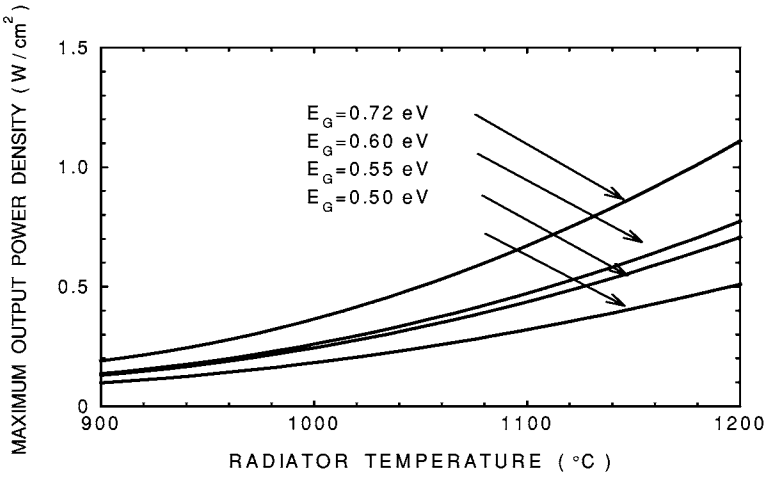

FIGURE 5. Maximum Output Power Density vs. Radiator Temperature

STRUCTURE OF QUATERNARY GaInAsSb TPV CELLS

The quaternary material was OMVPE grown lattice matched to GaSb.The typical structure of the TPV cell is a p-on-n configuration with a 1μm thick n-type GaInAsSb base layer doped to ~$5x10^{17}$ cm^{-3}, a 4 μm-thick GaInAsSb p-emitter

layer doped to ~$2x10^{17}$ cm^{-3} and a 0.05 μm GaSb window layer doped p-type to $2x10^{18}$ cm^{-3}. One of the advantages of the above structure is that there are window GaSb layers both at the top of the emitter and at the bottom of the base. Since the GaSb layers have a higher bandgap and doping concentration than the emitter and base layers, the main effect is to reduce the effective recombination velocity at the window layer-active layer interface.

SIMULATION OF GaInAsSb TPV CELLS

We have used PC-1D to simulate the performance of cells with the physical structure described above. In addition we have assumed that the GaSb layer below the cell base layer is 10 μm thick and we have assumed that the surface recombination velocity at the top and bottom GaSb window layers is 10^6 cm/sec. Also we have assumed that the lifetime of excess carriers due to SRH recombination is 1 millisec. These are the only two assumptions of the simulation, all the parameters of the GaInAsSb quaternary alloy have been obtained from the material parameters of the binaries GaAs, InAs, GaSb and InSb as described at the beginning of the paper. Figure 6 shows the results of the simulation and compares the experimentally measured external QE to the simulated one.

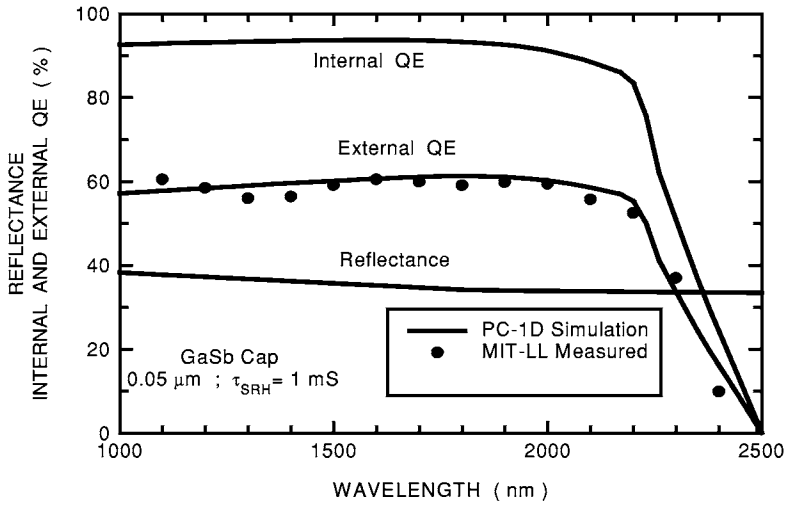

FIGURE 6. Simulated and Measured QE of GaInAsSb (0.55 eV) TPV Cell.

The agreement between the simulated and measured external QE is very good considering that the only parameters used in the simulation were the physical dimensions and doping concentration of the base and emitter layers. The excellent agreement at long wavelengths, above 2200 nanometers, is because we have

augmented the absorption constant calculated from the binaries by the absorption due to the Ürbach edge experimentally measured in this alloy (7).

Comparing this result with the external QE shown in Fig. 4 for a GaInSb TPV cell, we see that the advantage of the OMVPE grown TPV cell is to reduce the effect of the surface recombination velocity. This is caused by the presence of the window layers that because of their higher doping and larger energy bandgap effectively reduce surface recombination effects. Since the doping concentrations in the emitter and base are of the order of 10^{17} cm^{-3}, the lifetime is long enough that any carrier generated in the emitter or base is collected by the junction and not lost by bulk recombination. This makes the internal QE reach values close to 95 % and it could reach 100 % if the doping is lowered to ~ 10^{16} cm^{-3}.

In addition we have simulated the illuminated I-V characteristics of the above cell and are shown in Fig. 7 for a maximum short circuit current density of 3.5 A/cm^2 in order to compare them to the measured characteristics. The simulation gives an open circuit voltage of 0.279 V and the measured open circuit voltage for a current density of 3.5 A/cm^2 was 0.310 V. The difference of 31 mV could be to either inaccurate values used of the intrinsic concentration for the 0.55 eV quaternary alloy, or in the Auger and radiative recombination coefficients or to wrong values assumed for the doping concentrations. Considering that all the quaternary alloy parameters were obtained from the parameters for the binaries, the agreement is rather remarkable.

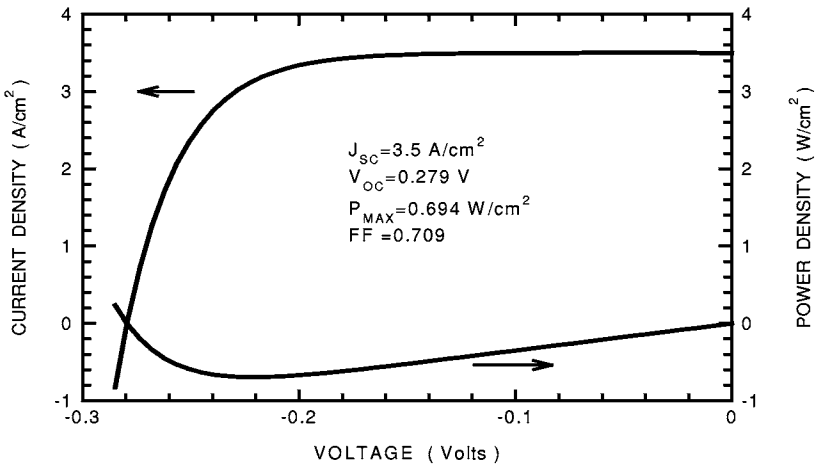

FIGURE 7. Simulated Light I-V Characteristics of GaInAsSb TPV Cell.

In addition we have simulated the performance of the above OMVPE quaternary cell as function of radiator temperature, as shown in Fig.5 for bulk diffused GaSb and GaInSb cells, and the results are given in Fig. 8. The results in the above figure show that the OMVPE quaternary cell outperforms all the other cells at all radiator temperatures simulated.

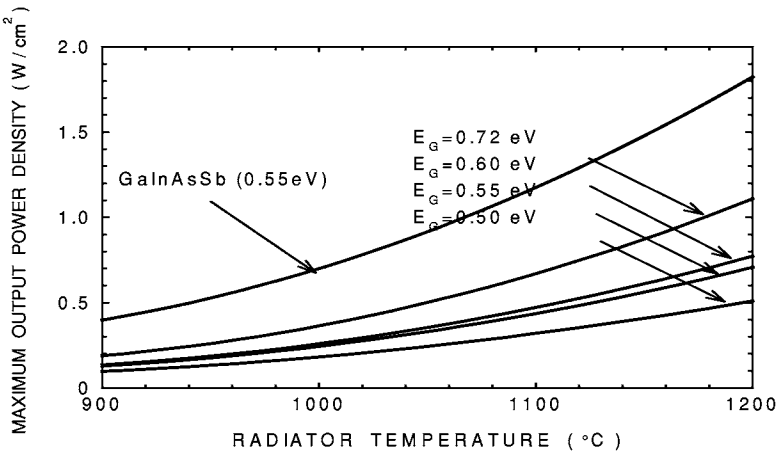

FIGURE 8. Maximum Output Power Density vs. Radiator Temperature

We believe the main reason for the performance advantage of the OMVPE GaInAsSb grown cell compared to the bulk diffused GaInSb is not so much to the material parameters since they have similar energy bandgap but to the structure of the cells. The bulk-diffused cells have a heavily doped emitter that does not collect photogenerated carriers very efficiently and the emitter behaves rather like a "dead layer" which contributes to the dark current. In addition the base is very long with short lifetime so carriers photogenerated a few microns from the junction are not confined to the base but can diffuse away from the junction and lost by bulk recombination. The OMVPE grown TPV cell has the important characteristic of incorporating window layers of wider bandgap and heavily doped material, both at the emitter and at the base, which help to confine the photogenerated carriers and are collected by the junction because of the long diffusion length compared to the size of the emitter and base regions. In addition the base and emitter regions are not heavily doped so the dark current contributed by these regions is reasonable small. This dark current could be further reduce by lowering the doping in emitter and base regions as long as there is an appreciable built in voltage for carrier collection. The performance advantage of the OMVPE quaternary cell over the bulk diffused GaSb and GaInSb depends upon other variables, like spectral control of the thermal radiation and cell AR coating, which has not been included in these simulations. Further improvement in any of the considered cells will change the performance advantage of the OMVPE quaternary cell over the bulk Zn diffused GaSb and GaInSb cells.

CONCLUSIONS

In this paper we have compared the performance of GaSb, GaInSb TPV cells fabricated by bulk diffusion to the performance of quaternary cells GaInAsSb

grown by OMVPE with similar bandgap as function of radiator temperature. The performance was obtained from simulation using PC-1D. The material parameters for the ternary and the quaternary alloys were derived from the material parameters of the binary materials GaAs, InAs, GaSb and InSb using well-known rules. The calculated mobility and optical absorption constants were compared with experimental measurements and reasonable agreement was obtained which gives confidence to the method employed for calculating the parameters of the alloys. The results of the simulation of the cells as function of radiator temperature show the superior performance of the quaternary OMVPE GaInAsSb TPV cell for radiator temperatures between 900°C and 1200°C .We believe this is due to the window layers in the emitter and base of the OMVPE quaternary cell that help to confine the photogenerated carriers.

REFERENCES

1. Madelung, O., Editor *Semiconductors Group IV and III-V Compounds*, Springer-Verlag 1991.

2. Wiley, J.D., in *Semiconductors and Semimetals*, Willarsdon, R.K and Beer, A.C. eds, vol. 10, Academic Press, New York 1975.

3. Hilsum, C. and Rose-Innes, A.C., *Semiconducting III-V Compounds*, Pergamon Press, New York 1961.

4. Milnes, A.G. and Polakov, A.Y., *Solid State Electronics*, **36**, 803-818, 1993.

5. -Adachi, S., *Optical Constants of Crystalline and Amorphous Semiconductors*, Kluwer Academic Publishers, Boston 1999.

6. Adachi, S., *Physical Properties of III-V Semiconductor Compounds*, John Wiley and Sons, New York 1992.

7. Munoz, M., Wei, K., Pollak, Fred H., Freeouf, J.L., Wang, C.A., Charache,G.W., *J. of App. Physics,* **87**, 1780-1787, (2000).

8.Grein, C.H., Young, P.M., Flattė, M.E. and Ehrenreich, H, *J. of App. Physics*, **78**,7143-7152, (1995).

9.Charache,G.W.,Baldasaro,P.F.,Danielson,L.R.,DePoy,D.M.,Freeman,M.J., Wang,A.C.,Choi,H.K.,Garbuzov,D.V.,Martinelli,R.U.,Khalfin,V.,Saroop,S., Borrego,J.M. and Gutmann,R.J.,*J.of App.Physics*,**85**,2247-2252,(1999).